X-ray Diffraction Analysis of Cytochrome P450 2B4 Reconstituted into Liposomes[†]

John P. Miller,[‡,§] Leo G. Herbette,[||] and Ronald E. White*[,⊥]

Department of Pharmacology and Biomolecular Structure Analysis Center, University of Connecticut Health Center, Farmington, Connecticut 06030, and Department of Metabolism and Pharmacokinetics, Bristol-Myers Squibb Pharmaceutical Research Institute, P.O. Box 4000, Princeton, New Jersey 08543-4000

Received June 27, 1995; Revised Manuscript Received October 10, 1995[⊗]

ABSTRACT: Two general models of the membrane topology of microsomal cytochrome P450 have been proposed: (1) deep immersion in the membrane, and (2) a $P450_{cam}$-like heme domain anchored to the membrane with one or two membrane-spanning helices. Lamellar X-ray diffraction of oriented membrane multilayers was employed to distinguish these alternatives. Cytochrome P450 2B4 was reconstituted into unilamellar phospholipid proteoliposomes (molar protein to lipid ratio 1:90). Sedimentation of the proteoliposomes produced an ordered stack of bilayers with a one-dimensional repeat distance (*d*) perpendicular to the plane of the bilayer. The stacked multilayers were exposed to an X-ray beam (λ = 1.54 Å) at near grazing incidence, and lamellar diffraction patterns were recorded. With proteoliposome multilayers, up to six diffraction orders could be observed. Their spacing corresponded to a *d* of 63.6 Å, calculated according to Bragg's Law, comprising the lipid bilayer, the projection of the incorporated protein beyond the bilayer, and the intermembrane water layer. With liposome multilayers containing no P450, the observed *d* was 59.6 Å. These data suggest that the increase of distance between successive bilayers in the stack due to the presence of P450 2B4 was only about 4 Å. This distance is much less than would be expected with the "*N*-terminal membrane-anchor" model of the membrane topology, in which the P450 molecules largely extend beyond the surface of the membrane (≥35 Å). Furthermore, the mass distribution deduced from Fourier synthesis confirms that the protein is deeply immersed in the membrane.

The association of microsomal cytochrome P450 and its redox partners, P450 reductase and cytochrome b_5, with the endoplasmic reticulum membrane has been widely investigated and discussed. All three proteins are tightly associated with the membrane, but both the reductase and b_5 can be removed in partially active form by brief exposure to trypsin. In both cases, a small hydrophobic tail is clipped from the main body of the protein, leaving the catalytic site intact. However, the membrane binding tail is apparently necessary for either protein to transfer electrons to P450. On the other hand, release of P450 from the membrane requires much more drastic proteolytic conditions, such that the enzyme is extensively fragmented. All three proteins can be isolated from the membrane in completely active form by gentle detergent solubilization. The picture that arose from these observations was that both the reductase and b_5 are attached to the membrane through a small hydrophobic peptide segment, while the hydrophilic bulk of both proteins sits atop the membrane (Ingelman-Sundberg, 1986). Cytochrome P450, on the other hand, was thought to lie deeply imbedded in the bilayer, its substrate binding site perhaps actually within the bilayer ("deep immersion" model).

Once the primary structure of P450 2B4[1] was known, predictions of secondary structure suggested as many as eight membrane-spanning α-helices (Heinemann & Ozols, 1982; Tarr *et al*., 1983), in accord with the deep immersion model. Later, a different approach to the tertiary structure, that of structural alignment of the homologous amino acid sequences of microsomal P450 and $P450_{cam}$, led to a model in which only two transmembrane helices served as a membrane anchor, while most of the bulk of the P450 protein lay outside the bilayer (Nelson & Strobel, 1988). Recently, the latter model was modified such that only one transmembrane helix was postulated (Edwards *et al*., 1991; Black *et al*., 1994). This may be called the "partial immersion" model.

A number of biochemical experiments relating to the membrane topology have been reported. Some appear to favor the partial immersion model, although not all point to the one-helix variation (Brown & Black, 1989; Kunz *et al*., 1991; Vergères *et al*., 1991; Uvarov *et al*., 1994; Black *et al*., 1994). On the other hand, at least one biochemical result seems to be in accord with the deep immersion model (Pernecky *et al*., 1995).

A few reports of physical measurements related to the association with the microsomal membrane have appeared. These have all involved rotational measurements, determined by EPR (Schwarz *et al*., 1990) or by absorbance depolarization (Kominami *et al*., 1993; Ohta *et al*., 1994). The

[†] This work was partially supported by Research Grant ES03600 (to R.E.W.) from the National Institutes of Health.

* Author to whom correspondence should be addressed. Telephone: (609)-252-4883. FAX: (609)-252-6802. E-Mail: white@bms.com.

[‡] Department of Pharmacology, University of Connecticut Health Center.

[§] Present address: American Red Cross Blood Services, 100 S. Robert St. St. Paul, MN 55107.

[||] Biomolecular Structure Analysis Center, University of Connecticut Health Center.

[⊥] Bristol-Myers Squibb Pharmaceutical Research Institute.

[⊗] Abstract published in *Advance ACS Abstracts,* January 15, 1996.

[1] Abbreviations: DPPC, dipalmitoylphosphatidylcholine; LUV, large unilamellar vesicles; P450 2B4, phenobarbital-inducible rabbit liver microsomal cytochrome P450 (CYP2B4 gene product; Nelson *et al*., 1993); $P450_{cam}$, soluble camphor-hydroxylating cytochrome P450 from *Pseudomonas putida*, systematic name P450 101; PC, egg yolk phosphatidylcholine; PE, phosphatidylethanolamine; PS, phosphatidylserine; RH, relative humidity; SUV, small unilamellar vesicles.

0006-2960/96/0435-1466$12.00/0

observations have been that the rotation was slow or that rotational properties were independent of the presence of the proposed membrane anchor of amino acids 2−30, consistent with protein molecules deeply imbedded in the membrane. Thus, while the rotational measurements provide only an indirect assessment of membrane topology, they offer little support for the partial immersion model.

The objective of this work was to directly measure the depth of insertion of the cytochrome P450 protein into a phospholipid bilayer similar to that of the endoplasmic reticulum. The general approach involved preparation of uniform proteoliposomes containing P450 incorporated in the bilayer. These proteoliposomes, which mimic the association of P450 with the physiological membrane, can be sedimented into stacked planar bilayers and subjected to low-angle X-ray diffraction. The resulting one-dimensional unit-cell information provides a direct physical measurement of the maximum distance that the protein could project into the intermembrane space. In addition, the electron density profile, derived from Fourier analysis, indicates the distribution of lipid and protein mass across the width of the membrane.

MATERIALS AND METHODS

General Analytical Procedures. Phospholipid purity was analyzed by TLC (Skidmore & Entenman, 1962) and HPLC (Geurts Van Kessel *et al*., 1977). Phospholipid stock solutions were prepared in chloroform and stored at −20 °C until use. The phospholipid concentrations of the stock solutions were determined by phosphate analysis according to the phosphomolybdate method (Chen *et al*., 1956). For analysis of the lipid content of membrane multilayers, the lipid was extracted overnight with chloroform (3 × 1 mL). The protein in the multilayer was solubilized in 1 mL of 1% sodium dodecyl sulfate containing 0.1 M NaOH.

Cytochrome P450 concentrations were determined from absorbance spectra with sample buffer in the reference cuvette. For light-scattering samples (*e.g*., liposomes), the absorbance difference (418−500 nm, ferric state) was used to calculate cytochrome P450 concentrations, with a molar absorptivity of 91 mM^{-1} cm^{-1} determined in this laboratory. For optically clear solutions, a molar absorptivity of 110 mM^{-1} cm^{-1} was applied to the absolute absorbance at 451 nm with buffer in the reference cuvette (White & Coon, 1982).

Chemicals. All nonradiolabeled lipids were from Avanti Polar Lipids (Birmingham, AL). Cholic acid was recrystallized from ethanol/water. [^{14}C]DPPC was obtained from Amersham (Arlington Heights, IL). [^{3}H]Cholic acid (specific activity 50 Ci/mmol, DuPont NEN, Boston, MA) was purified to radiochemical homogeneity by HPLC on a Brownlee Aquapore C8 column (4.6 mm × 22 cm) with a mobile phase containing acetonitrile/10 mM potassium phosphate, pH 7.5 (20:80). Amberlite XAD-2 was obtained from Sigma Chemical Co. (St. Louis, MO). Sephacryl HR-400 and Blue Dextran were obtained from Pharmacia (Piscataway, NJ).

Preparation of Cytochrome P450 2B4. Rabbit liver cytochrome P450 2B4 ($P450_{LM2}$; official name CYP2B4; Nelson *et al*., 1993) was prepared by the general method outlined by Coon *et al*. (1978), with modifications (McCarthy & White, 1983). In the final electrophoretically homogeneous preparation, the ratio of the absorbance at 418 nm to 280 nm (R_Z number) was 1.53, indicating a high content of holoenzyme with little residual detergent. The specific heme content of the protein was 16.6 nmol of P450/mg of protein, compared to the theoretical value of 17.9 nmol of P450/mg of protein based on the enzyme molecular weight of 55 800. The absorbance spectrum of the ferrous carbonyl derivative indicated intact P450 free of P420.

Preparation of Proteoliposomes. Cytochrome P450 2B4 was incorporated by cholate dialysis into unilamellar liposomes consisting of a mixture of egg yolk phosphatidylcholine, phosphatidylethanolamine, and bovine phosphatidylserine by a modification of the method of Gut *et al*. (1982). In cases where lipid radioactivity was desired for monitoring purposes, [^{14}C]DPPC was also used. All buffers were bubbled with nitrogen to retard lipid oxidation. A chloroform solution containing PC/PE/PS (11:5:2) was dried under a gentle stream of nitrogen and lyophilized overnight. The lipid was bath-sonicated for several minutes until clear in cholate buffer containing 250 mM HEPES, pH 7.4, 5.6% sodium cholate, and 20% glycerol to yield a final lipid concentration of 10 mg/mL. P450 2B4 (10 mmol, 0.27 mL), lipid−cholate buffer (0.066 mL, 660 μg of lipid), and lipid-free cholate buffer (0.034 mL) were incubated overnight at 4 °C or at room temperature for 3 h. The mixture of protein and lipid was dialyzed for 3 h at room temperature against 200 volumes of buffer containing 20 mM HEPES, pH 8.0, 1 mM EDTA, Amberlite XAD-2 (10 g/L), and 20% glycerol (dialysis buffer). The buffer was changed once after 90 min. The proteoliposomes that formed were further dialyzed against 1 L of dialysis buffer overnight at 4 °C. For preparations that were to be submitted for X-ray analysis, glycerol was omitted from the final dialysis buffer. These proteoliposomes contained 0.67% of the initial cholate, for a final cholate to lipid ratio of 1:10. Proteoliposomes were stable for at least 4 days when stored at either 4 or 24 °C.

Characterization of Proteoliposomes. Isopycnic centrifugation of [^{14}C]DPPC-containing vesicles was performed in 20−80% glycerol gradients containing 20 mM HEPES, pH 8.0, and 0.1 mM EDTA throughout. The vesicles were diluted 1:1 with non-glycerol dialysis buffer. The vesicles were loaded on top of the glycerol gradients, which were centrifuged at 105000*g* for 15 h at 10 °C. The gradients were eluted by puncturing the bottom of the centrifuge tube with a needle.

Gel filtration of the vesicles was performed on a column of Sephacryl HR-400 (1.6 cm × 12 cm). The column was loaded with a sonicated suspension of P450 (20 nmol) and PC (2 mg) to prevent adsorption of vesicle lipid and protein onto the column. The column was equilibrated with 5 volumes of 20 mM HEPES, pH 8.0, 0.1 mM EDTA, and 20% glycerol (running buffer). Vesicle preparations of varying P:L ratios containing 15 nmol of P450 in approximately 0.5 mL were loaded, and proteoliposomes were eluted with running buffer at a flow rate of 10 mL/h.

Vesicles for electron microscopy were fixed in a solution of 1.25% glutaraldehyde in 0.1 M cacodylate buffer, pH 7.4, for 1 h at room temperature. The fixed vesicles were pelleted by centrifugation at 40000*g* for 20 min, and the supernatant was discarded. The pellet was rinsed in 0.1 M cacodylate buffer, pH 7.4 (3 × 15 min), and fixed in a solution of 1.0% OsO_4 in 0.1 M cacodylate for 1 h on ice in the dark. After a water rinse, the pellet was stained with a solution of 0.25%

uranyl acetate for 1 h on ice in the dark. Dehydration of the pellet was accomplished by successive 15 min incubations in 70% ethanol, 95% ethanol, and 100% ethanol (×2). The pellet was infiltrated with propylene oxide/Poly-Bed 812 (3:1) for 15 min, 1:1 for 30 min, 1:3 overnight, and 100% Poly-Bed 812 for 1 h under vacuum. Polymerization occurred at 60 °C overnight. The embedded sample was sectioned with a LKB Nova microtome. Microscopy was performed on a Phillips CM 10 electron microscope.

X-ray Diffraction of Membrane Multilayers. (A) Preparation of Multilayers. Membrane multilayers were formed by sedimentation of proteoliposomes (5 nmol of P450 and 330 μg of phospholipid) onto aluminum foil in Lucite sedimentation cells at 10000*g* for 1.5 h in a Beckman SW 28 swinging-bucket rotor, as described previously (Herbette *et al*., 1977). The foils were mounted on curved glass supports. The pellet was equilibrated at least 12 h over saturated salt solutions that provided a specific RH (81−93%). Samples were mounted in sealed brass canisters containing the appropriate saturated salt solution to maintain a constant RH. Aluminum foil windows in the canisters allowed passage of the X-ray beam.

(B) X-ray Diffraction. The brass canisters containing the sample were placed in a refrigerated holder to maintain the temperature at 10 ± 1 °C. The multilayer was exposed to a monochromatic, collimated X-ray beam emitted from a Rigaku-Denki RU3 rotating copper anode generator and brought to a line focus by a diffraction camera containing a single vertical Franks' mirror to enhance the monochromaticity of the beam (Herbette *et al*., 1977). The slit height of 1 mm produced reflection arcs that were approximately 75% of the acceptance window of the X-ray detector, so that the entire reflection would be integrated by the detector, eliminating the need for an additional factor of *s* beyond the single *s*-factor for the Lorentz correction. The X-ray wavelength was 1.54 Å (CuK_α). The sample was oriented approximately 40% into the beam at near grazing incidence to obtain optimal lamellar diffraction. Diffraction patterns were recorded for approximately 1 h with a one-dimensional quartz wire detector (Braun) or overnight on X-ray film (Kodak NS5T).

Data Analysis. The membrane unit cell dimension (*d*) was calculated from the spacing between adjacent diffraction orders and the sample to detector distance (163 mm). Linear distances between diffraction orders were obtained from the difference in detector channel numbers with the conversion factor of 31 channels/mm. The digitized reflection peaks were base-line-corrected, integrated, and corrected by a factor of $s = \sin\theta/\lambda$ (Herbette *et al*., 1977). Fourier synthesis was accomplished as outlined by Franks and Lieb (1981). Structure factors [$F(h) = \pm\sqrt{I(h)}$ where $I(h)$ is the integrated intensity of the hth reflection] were assigned phases by calculation of electron density profiles for all possible phase combinations and retaining those that corresponded to physically real possibilities. Five reflections were used for analysis of proteoliposomes, giving a resolution (d/h_{max}) of 13 Å, but only three were available for liposomes, giving a resolution of 20 Å. Relative values of the electron density function, $\rho(x)$, were calculated by a Fourier series:

$$\rho(x) = \sum_{h=1}^{h_{max}} F(h) \cos(2\pi hx/d)$$

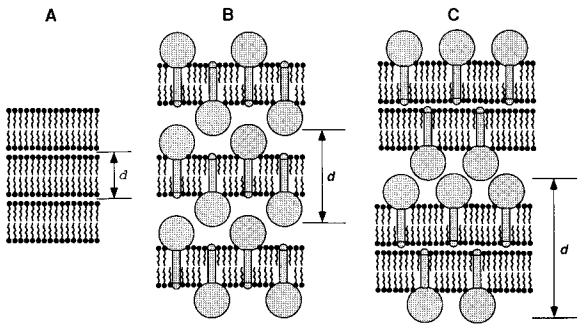

FIGURE 1: Schematic diagram of stacked bilayers resulting from sedimentation of liposomes. Panels represent multilayers from (A) liposomes, (B) proteoliposomes with symmetric protein incorporation, and (C) proteoliposomes with asymmetric protein incorporation.

RESULTS

Structure of Stacked Multilayers. Ultracentrifugation of a suspension of liposomes produces a stack of bilayers, formed by the collapse of liposomes as they sediment to the bottom of the centrifuge cell. The resulting stacked multilayer presents an ordered array with a one-dimensional repeat distance (*d*) perpendicular to the plane of the bilayer and equal to the basic symmetric unit (Figure 1; Herbette *et al*., 1977). If the liposomes contain only lipid with no incorporated protein, then the symmetric unit will be a single bilayer along with the associated water between successive layers. If the liposomes contain bilayer-associated protein (*i.e*., proteoliposomes), the symmetric unit will be a single lipid bilayer if the protein was incorporated symmetrically into the membrane, or two lipid bilayers if the protein was incorporated asymmetrically. In either case, *d* will approximately equal the sum of the thickness of the bilayer(s), the extent of protrusion of protein beyond the lipid bilayer, and the thickness of the intermembrane water layer, which depends upon the relative humidity.

Proteoliposome Formation. For the purpose of X-ray diffraction of stacked multilayers, proteoliposomes had to be unilamellar and contain a molar protein-to-lipid ratio (P:L) of at least 1:100 (mol/mol). Attempts to circumvent the use of cholate and incorporate high levels of cytochrome P450 2B4 into preformed liposomes prepared either by reverse phase evaporation (Szoka *et al*., 1980) or by sonication followed by purification (Barenholtz *et al*., 1977) were unsuccessful. We were able to incorporate adequate levels of protein using the cholate dialysis method described by Gut *et al*. (1982), but these vesicles precipitated upon removal of glycerol. However, increasing the proportion of phosphatidylserine in the vesicle preparation from 6.7% to 8%, which increased the overall negative charge, allowed removal of glycerol without vesicle aggregation. Our final procedure used a 11:5:2 molar mixture of PC, PE, and PS, approximating the relative abundance of these lipids in microsomes (DePierre & Dallner, 1975). After optimization of the lipid composition, systematic variation of the P:L ratio from 1:128 to 1:64 revealed that the maximal ratio that maintained vesicle integrity without aggregation was 1:85, corresponding to a mass ratio of about 1:1. The structural integrity of vesicular P450 at these P:L ratios was proven by the retention of the characteristic carbon monoxide binding spectrum in the final proteoliposome preparation. For comparison, rat liver microsomes have a P:L ratio of

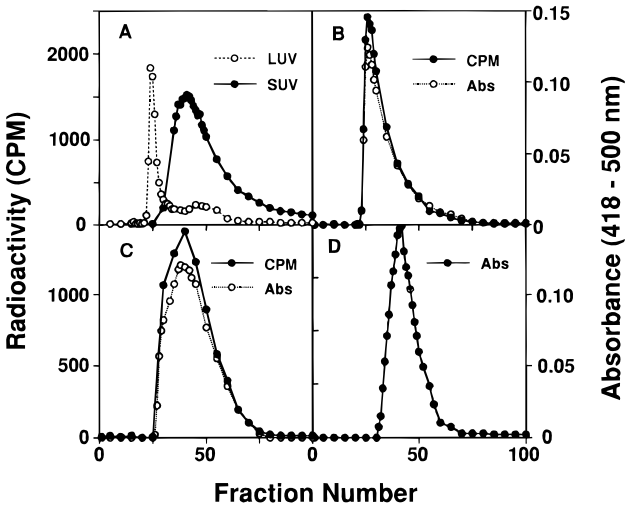

FIGURE 2: Gel filtration of proteoliposomes: Samples were eluted from a Sephacryl HR-400 column, as described under Materials and Methods. (A) Calibration of column with SUV and LUV. (B) Elution of 1:85 proteoliposomes. (C) Elution of a nonvesicular preparation with a protein to lipid molar ratio of 1:42. (D) Elution profile of P450 alone, in the absence of lipid. As additional calibration, cuprous ion (diameter <10 Å) and Blue Dextran (ave MW 2×10^6) eluted in fractions 55 and 44, respectively (profiles not shown). P450 was measured by the absorbance difference between 418 and 500 nm. Lipid was determined as [^{14}C]DPPC.

1:23, a number that includes all microsomal proteins, not only P450 (DePierre & Dallner, 1975). Because it was important that these heavily protein-loaded liposomes be intact and unilamellar, they were further characterized as described below.

Isopycnic Ultracentrifugation. Reconstitution of protein and lipid by cholate dialysis in P:L ratios of 1:170, 1:85, and 1:42 was monitored by isopycnic ultracentrifugation in 20−80% glycerol gradients. For the 1:170 and 1:85 samples, the protein and lipid coeluted in sharp bands of average density 1.092 and 1.107 g/mL, respectively. These values are similar to the value of 1.093 g/mL for 1:150 P:L vesicles shown by Bosterling *et al*. (1979). In contrast, the elution of the 1:42 sample showed a broad elution of protein and lipid indicative of an inhomogeneous, nonvesicular preparation. Pure protein and pure lipid appeared at the bottom and top of the gradient, respectively.

Gel Filtration. Further demonstration of successful incorporation of protein into liposomes and determination of the size distribution of the resultant proteoliposomes was accomplished by gel filtration. In order to estimate the size of the proteoliposomes, the column was calibrated with LUV having an average diameter of 1000 Å and SUV having an average diameter of approximately 300 Å (Figure 2A), prepared by the method of Enoch and Strittmatter (1978). The elution peaks of the proteoliposomes (Figure 2B) and LUV nearly coincide at fractions 26 and 24, respectively. The broader elution of the proteoliposomes compared with the LUV suggested a minority of the proteoliposomes had diameters extending down into the SUV range. A control preparation containing nonvesicular protein and lipid in a 1:42 ratio had a distinctly different, broader elution profile with peak elution occurring at fraction 36 (Figure 2C). The proteoliposome preparation did not contain an appreciable fraction of unincorporated protein, which eluted maximally at fraction 42 (Figure 2D).

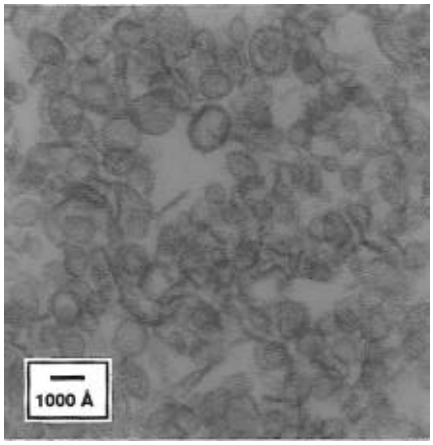

FIGURE 3: Electron microscopy of proteoliposomes. Sample prepared as described under Materials and Methods with P:L ratio = 1:85. The black bar represents 1000 Å.

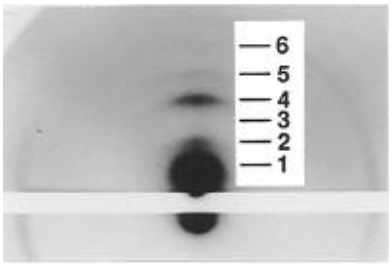

FIGURE 4: Film pattern from lamellar X-ray diffraction of proteoliposome-derived multilayer at 88% RH. Multilayer preparation and X-ray diffraction were performed as described under Materials and Methods. The diffraction pattern was recorded on X-ray film. The assigned diffraction orders ($h = 1-6$) are indicated. The calculated d was 62 Å.

Electron Microscopy. The diameter of the proteoliposomes as well as the lamellar structure of the vesicle membrane was evaluated by electron microscopy. As can be seen in Figure 3, the vesicles were unilamellar with no contamination by multilamellar vesicles. In addition, the proteoliposomes ranged from 500 to 1300 Å in diameter with an average diameter of *ca*. 1000 Å, in agreement with the gel filtration results. The thickness of the unilamellar membrane was approximately 70 Å.

X-ray Diffraction of Multilayers. Membrane multilayers were prepared from the proteoliposomes by sedimentation onto aluminum foil followed by equilibration to a selected RH (Herbette *et al*., 1977). This stack of parallel lamellae provided the repeating structural unit necessary for low-angle X-ray diffraction. Starting from Bragg's Law, one can show that the thickness of this membrane unit cell is inversely proportional to the spacing between diffraction orders:

$$d = h\lambda a/b$$

In this expression, h is the diffraction order, λ is the X-ray wavelength, d is the one-dimensional unit cell repeat distance, a is the sample to detector distance, and b is the distance at the detector between diffraction orders (Franks & Lieb, 1981).

The lamellar diffraction pattern of the cytochrome P450 2B4 multilayer equilibrated at 88% RH was initially recorded on film (Figure 4). The overall appearance is similar to previously published diffraction patterns. The film pattern showed a series of diffraction arcs with a large first diffraction order, a much smaller second order, and a

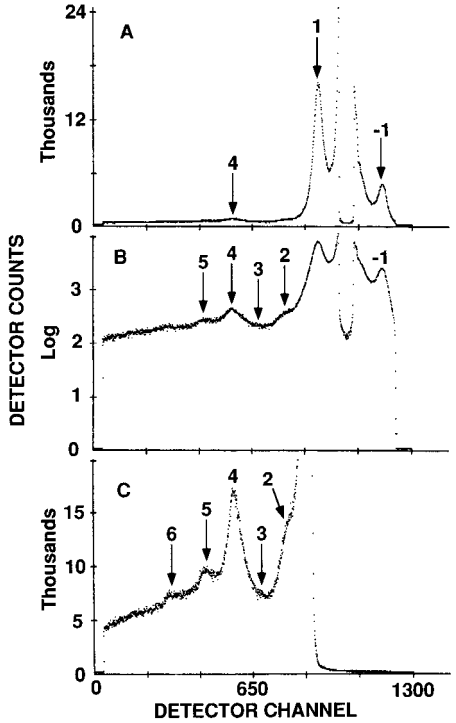

FIGURE 5: Lamellar X-ray diffraction of proteoliposome-derived multilayer at 88% RH. The sample was the same as in Figure 4, except that the diffraction pattern was recorded by means of a quartz wire detector. Accumulated counts as a function of detector channel number are shown. The assigned diffraction orders ($h = 1-6$) are indicated. (A) Full-scale one-dimensional detector pattern. (B) Replot of pattern in frame A on a logarithmic scale to facilitate visualization of higher order reflections. (C) Pattern obtained by blocking the first order band with a lead shield during diffraction to enable greater acquisition of signal for the higher order reflections. The calculated *d* was 63.6 Å.

prominent fourth order. The near-zero intensity at $h = 3$ represents a node, which is common in such patterns (Franks & Lieb, 1981). Careful examination reveals arcs corresponding to $h = 5$ and 6. The calculated *d*-space was about 62 Å. The film shown in Figure 4 was heavily overexposed in the first order region to reveal the higher order reflections. A ring near the periphery of the pattern is a camera artifact due to scattering off the aluminum foil surfaces and different sizes for the entrance and exit windows and is not related to the sample. An apparent additional reflection just beyond the $h = 6$ reflection is merely the continuation of the ring across the top of the sample and is not a seventh diffraction order.

For a more definitive analysis, this pattern and subsequent patterns were also recorded on a quartz wire detector (Figure 5A). The second diffraction order was not seen as clearly on the wire detector as it was on the film. When the pattern was displayed on a logarithmic scale (Figure 5B) or when the large first order reflection was blocked to enable the accumulation of more detector counts in the higher order region (Figure 5C), a total of six diffraction orders were seen ($h = 1-6$). The spacing between these reflections corresponds to an average *d*-space of 63.6 Å. For comparison, the diffraction pattern of a control multilayer composed of lipid alone with no P450 is shown in Figure 6. Three diffraction orders ($h = -1, 1, 2$) are easily observable, with an average *d*-space of 59.6 Å. A very weak $h = 3$ reflection is also present. This *d* agrees well with results from the phospholipid membrane from cardiac sarcoplasmic reticulum,

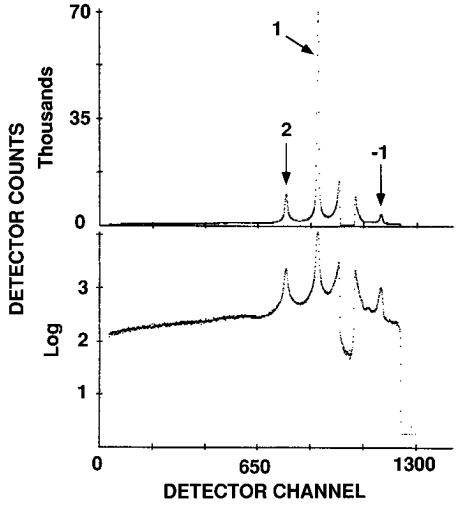

FIGURE 6: Lamellar X-ray diffraction of liposome-derived multilayer at 88% RH. (A, top panel) Pattern obtained from a multilayer consisting of lipid alone, with no P-450 present. (B, bottom panel) Logarithmic scale. The calculated *d* was 59.6 Å.

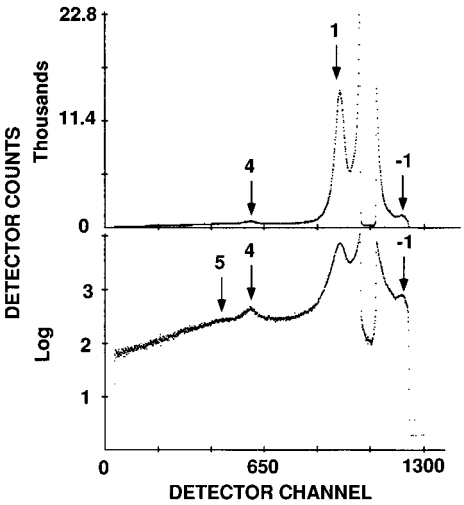

FIGURE 7: Lamellar X-ray diffraction of proteoliposome-derived multilayer at 81% RH. (A, top panel) Complete one-dimensional detector pattern. (B, bottom panel) Logarithmic scale. The calculated *d* was 62.7 Å.

which had a unit cell thickness of *ca*. 60 Å (Herbette *et al*., 1983). Endoplasmic reticulum membranes are estimated to be 50−80 Å thick by electron microscopy (DePierre & Dallner, 1975).

Diffraction patterns were also obtained of multilayers equilibrated at different RHs. The pattern for the proteoliposome-derived multilayer equilibrated at 81% RH is shown in Figure 7. The pattern is very similar to that obtained at 88% RH. In fact, the peak positions are superimposable. The corresponding lipid-alone multilayer pattern is shown in Figure 8. At the lower humidity, the lipid-alone pattern noticably changed from that at 88% RH. The $h = 3$ reflection is clearly evident, and simple peak alignment shows that *d* has changed. The relationship between the *d*-values of the protein/lipid and lipid-alone multilayers at various RHs is seen in Table 1. The small difference between protein-loaded and control multilayer *d*-values (4 Å at 88% RH) indicates that the presence of P450 in the multilayer only minimally affected the repeat distance. The decrease in *d* at lower RH in the control multilayers corresponds to a decrease in the water space between

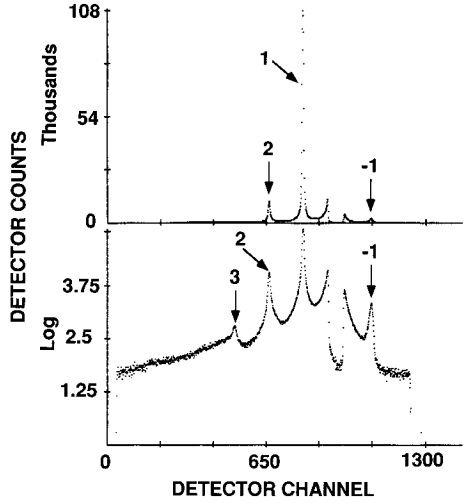

FIGURE 8: Lamellar X-ray diffraction of liposome-derived multilayer at 81% RH. (A, top panel) Pattern obtained from a multilayer consisting of lipid alone, with no P-450 present. (B, bottom panel) Logarithmic scale. The calculated *d* was 55.2 Å.

Table 1: Multilayer Repeat Distance as a Function of Relative Humidity

	d (Å)		
RH (%)[a]	proteoliposomes[b]	liposomes[c]	Δ*d* (Å)[d]
81	62.7	55.2	7.5
84	64.0	56.9	7.2
88	63.6	59.7	4.0
93	62.8	63.7	−0.9

[a] Controlled as described under Materials and Methods. [b] Multilayers prepared from liposomes with incorporated P450. [c] Multilayers prepared from liposomes containing no P450. [d] Difference in *d* between proteoliposome- and liposome-derived multilayers.

bilayers. The *d*-value of the P450-loaded multilayer, however, showed little change as a function of RH. In contrast, *d* for b_5-loaded multilayers changed from 145 to 163 Å when the RH was increased from 88% to 96% (Rzepecki *et al*., 1986). The lack of change with altered humidity of the P450 multilayers is not understood but may reflect interactions between P450 molecules in successive membranes, tending to maintain a fixed contact distance, or occupancy of the intermembrane space mainly by protein rather than water.

The small number of diffraction orders observed as well as their relative broadness in both the protein/lipid and lipid-alone diffraction patterns reflects some degree of membrane disorder, presumably resulting from residual cholate. At the conclusion of the diffraction experiments, the protein multilayer was analyzed for protein and lipid and found to have a molar P:L ratio of 1:91, in excellent agreement with the P:L ratio in the proteoliposomes used to prepare the multilayer (1:90).

Electron Density Profiles. The diffraction patterns obtained at 88% RH for both liposomes and proteoliposomes were transformed to one-dimensional electron density profiles by Fourier synthesis, as described under Materials and Methods. Values of the structure factors derived from reflection intensities are provided in Table 2. The principal problem in such an analysis is assigning proper phases to the structure factors. The usual procedure of swelling analysis at several RHs was not possible with the P450 proteoliposomes, since essentially no swelling occurred at higher humidities. Thus, our only option was to calculate

Table 2: Corrected Structure Factors and Viable Phase Combinations

	F(*h*)[a]	
h	liposomes	proteoliposomes
1	62.90	51.45
2	35.04	10.75
3	2.06	3.37
4		22.85
5		11.58
	viable phase combinations	
	$\pi\pi 0$	$\pi 00\pi 0$
	$\pi\pi\pi$	$\pi 0\pi\pi 0$
		$\pi\pi 0\pi 0$
		$\pi\pi\pi\pi 0$
		$\pi\pi 0\pi\pi$
		$\pi\pi\pi\pi\pi$

[a] For both proteoliposomes and liposomes, the sum of the structure factors are arbitrarily normalized to 100.

electron density profiles for all possible phase combinations. The number of combinations of 0 and π phases is given by 2^{h-1} where *h* is the number of orders used in the synthesis (Pachence *et al*., 1979). Our criteria for acceptance of a calculated pattern as "real" were (a) the center of the unit cell ($x = 0$ Å) must contain a clear minimum, corresponding to the low-density region between the ends of the alkyl chains of the phospholipids in the bilayer; and (b) clear maxima must be seen at $x = \pm 20-25$ Å, corresponding to the phosphate headgroups. These criteria represent the usual features of one-dimensional electron density profiles of phospholipid bilayers (Franks & Lieb, 1981).

First, the pattern from the liposome-derived multilayer was analyzed. Although swelling analysis was possible with these multilayers, we calculated all phase combinations anyway, since there were only four with $h = 3$. Two of these (π 0 0 and π 0 π) did not meet either of the acceptance criteria and were rejected. The remaining two (π π 0 and π π π) were nearly identical, since the $h = 3$ is weak and does not substantially contribute to the pattern (Table 2). The electron density profile (π π 0) for liposome-derived multilayers is shown in Figure 9A. It displays the classical lipid profile, with a trough at $x = 0$ and maxima at $x = \pm 20$ Å, indicating that the phosphate-to-phosphate distance across the bilayer is about 40 Å, a typical value for PC membranes.

Next, the pattern from the proteoliposome-derived multilayers was analyzed. We did not consider the intensity of the $h = 6$ reflection to be reliable due to interference from the generalized background signal. Therefore, we used 5 reflections in the analysis, giving 16 possible combinations of 0 and π. After Fourier synthesis of all 16 combinations, inspection showed that only those with the π phase for the $h = 4$ reflection corresponded to physically real situations. Since the $h = 3$ intensity was nearly zero, the eight patterns with π for $h = 4$ amount to four pairs with nearly identical members within each pair. One of the pairs (π 0 0 π π and π 0 π π π) produces a profile lacking a phosphate maximum and was rejected. The three remaining pairs are qualitatively the same as one another and could not be discriminated further (Table 2). One example from each pair is shown in Figure 9. These three pairs have several common features. First, each of these electron density profiles corresponds to a single-bilayer lipid profile with clear phosphate maxima.

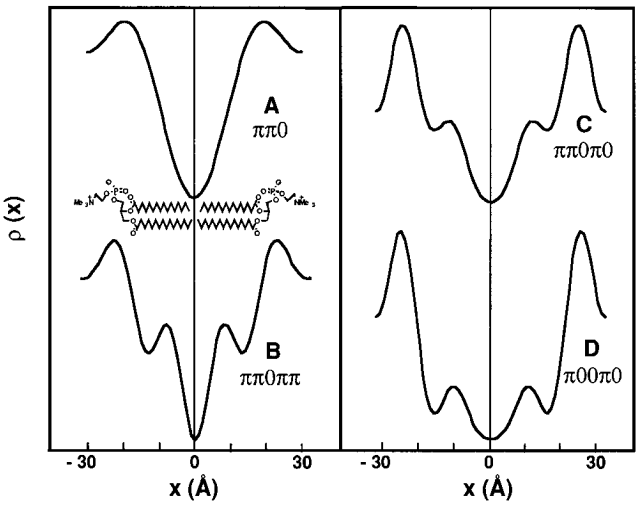

FIGURE 9: Electron density profiles. The relative electron density on an arbitrary scale is plotted as a function of distance *x* from the center of the bilayer. One unit cell is shown in each case. For orientation, two phosphatidylcholine molecules from the bilayer are aligned on the liposome profile. (A) Liposome-derived multilayer at 88% RH, $d = 59.6$ Å, phase combination $\pi\pi 0$. (B) Proteoliposome-derived multilayer at 88% RH, $d = 63.6$ Å, phase combination $\pi\pi 0\pi\pi$. (C) Proteoliposome-derived multilayer, phase combination $\pi\pi 0\pi 0$. (D) Proteoliposome-derived multilayer, phase combination $\pi 00\pi 0$.

Second, none exhibit any electron density maxima outside the bilayer region. Thus, no protein substantially protrudes from the bilayer. Third, the separation of phosphate headgroups across the bilayer ranges from 46 to 51 Å, while that of the pure lipid bilayer was 40 Å. Thus, incorporated protein must reside within the bilayer, in effect swelling the membrane. Fourth, all three profile pairs display electron density peaks within the hydrocarbon core structure. The structural significance of these peaks is not certain, since artifactual peaks due to Fourier truncation errors are possible at the limited resolution achieved in this experiment. However, it is also possible that these peaks represent protein-associated mass. In contrast, the electron density profile for cytochrome b_5 shows a phosphate-to-phosphate separation of 33 Å, with a second maximum about 18 Å beyond the headgroups, corresponding to the heme domain located *outside* the bilayer (Rzepecki *et al*., 1986). Thus, the P450 2B4 pattern is distinctly different from those of both lipid and b_5.

DISCUSSION

The lamellar X-ray diffraction technique employed in this study appeared to be ideal for detecting substantial segments of membrane-bound protein that project outside the lipid bilayer. The method has been previously applied to several other integral membrane proteins. For instance, the intact rabbit skeletal muscle sarcoplasmic reticulum (SR) contains mainly a large Ca/Mg-ATPase protein (102 kDa) that extends beyond the lipid bilayer by at least 25 Å, as well as having significant mass within the bilayer. In multilayers prepared from SR membranes, the unit cell consisted of two lipid bilayers with $d = 153-173$ Å (Herbette *et al*., 1977). Similarly, canine cardiac sarcolemmal membrane lipids alone have $d = 60$ Å, but the total thickness increased to *ca*. 77 Å when the sarcolemmal proteins were present, which can be seen in the electron density profile to protrude about 20 Å beyond the phosphate headgroups of the lipid bilayer (Herbette *et al*., 1985). Conversely, phosphatidylcholine liposomes containing bacterial photosynthetic reaction center protein had a membrane thickness of 58−62 Å, similar to that of the phosphatidylcholine alone, which was 50−60 Å, depending on the RH (90−95%) (Pachence *et al*., 1979). Since incorporation was asymmetric, the unit cell consisted of two lipid bilayers and *d* was 125−130 Å, approximately double the lipid membrane thickness. The electron density profile confirmed that the protein itself was essentially completely contained within the lipid bilayer.

The most appropriate comparison, however, can be made to the incorporation of cytochrome b_5 into liposomes. There is little doubt that the heme domain of b_5 is anchored to the membrane by a hydrophobic *C*-terminal 40-amino acid peptide segment [see Arinç *et al*. (1987) and references cited therein]. Stacked multilayers prepared from b_5-loaded proteoliposomes showed a repeat distance of 145−175 Å, depending on the RH at which they were equilibrated (Rzepecki *et al*., 1986), corresponding to a unit cell comprised of a centrosymmetric pair of bilayers. Thus, allowing 60 Å for each lipid bilayer, the unit cell was 25−55 Å wider than the sum of the bilayers. In fact, the electron density profile at 15 Å resolution clearly showed extra protein mass that projected beyond the phosphate headgroups by at least 18 Å.

It is clear from these examples that, in cases where an integral membrane protein extends appreciably beyond the lipid bilayer, a substantial increase in *d* beyond that of the lipid bilayer itself is observed. The three P450 enzymes for which the three-dimensional structures are known by X-ray crystallography (*i.e*., $P450_{cam}$, $P450_{terp}$, and the hemoprotein domain of $P450_{BM3}$) each have a triangular prism shape about 35 Å thick and 65 Å on each side (Hasemann *et al*., 1995). In the case of microsomal P450, then, the shallow immersion model predicts that successive lipid bilayers in the stacked multilayers would be separated by at least one P450 thickness (*ca*. 35 Å), and the measured value of *d* would have been at least 95 Å. Thus, at the molar ratio at which the P450 was reconstituted, the modest increase of *d* in our P450 2B4-loaded proteoliposomes strongly indicates that the majority of the protein must reside *within* the lipid bilayer. This conclusion is strengthened by the observation in the electron density profile of extra peaks deep in the bilayer and the lack of protein-associated peaks outside the bilayer. It should be noted that this conclusion should not be construed as confirmation of the protein folding scheme presented in the deep immersion models of Heinemann and Ozols (1982) and of Tarr *et al*. (1983). It may be possible for P450 2B4 to conform to the "P450 fold" pattern (Hasemann *et al*., 1995) and still be deeply immersed in the membrane.

We are not the first to propose a deep immersion topology for membrane-bound P450. For example, Seybert *et al*. (1979) concluded that adrenal mitochondrial $P450_{scc}$ is submerged in the bilayer on the basis of cholesterol accessibility to the enzyme active site in proteoliposomes, and a deep immersion topology is now generally accepted for the mitochondrial P450s (Takemori & Kominami, 1984). Two other adrenal enzymes, $P450_{C21}$, and $P450_{17\alpha,lyase}$, were characterized as deeply imbedded by their resistance to trypsinolysis. Furthermore, the rotational relaxation time of trypsin-treated protein was the same as that of untreated, indicating that the protein was not attached by a small hydrophobic anchor, but was instead deeply imbedded in the

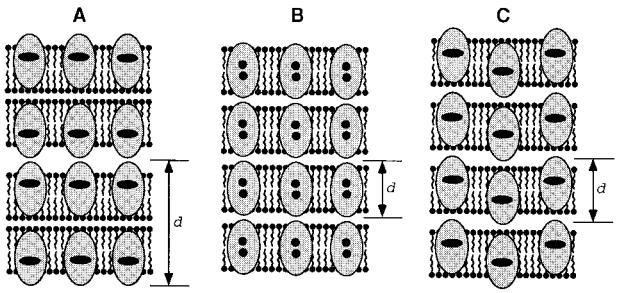

FIGURE 10: Schematic diagram of deep immersion topologies (not to scale). The large gray ellipses represent P450 protein. The small black ellipses or circles represent an electron-dense structural feature of the P450 protein. Panels represent multilayers from (A) asymmetric incorporation of P450 into liposomes. More of the P450 mass is on one side of the bilayer than the other. (B) Pseudosymmetric incorporation. While the P450 amino acid sequence has the same directionality within any single bilayer, the *mass* distribution is nearly symmetrical due to the deep immersion. (C) Symmetric incorporation. More of the mass of any one P450 molecule is on one side of the bilayer than the other, but the protein entered the bilayer from both sides during incorporation.

membrane (Kominami *et al*., 1993). Similarly, the rotational diffusion of expressed P450 1A1 in yeast microsomes was independent of the presence of the proposed membrane anchor of amino acids 2−30 (Ohta *et al*., 1994). In addition, the association of various truncated forms of P450 2B4 and 2E1 with membrane fractions from *E. coli* suggested that the proposed *N*-terminal segment was not uniquely involved in membrane attachment (Pernecky *et al*., 1993). Each of these results was in accord with the deep immersion model and was so interpreted in the cited works.

One conceivable way for the protein-containing multilayers to have only a slight increase in thickness compared to the lipid-only multilayers is that we achieved insufficient protein loading for the protein to have more than a local effect on membrane thickness. Thus, in this scenario, large areas of the membrane might form a coherent domain of pure lipid bilayer between widely separated P450 molecules. This possibility can be dismissed in two ways. First, in the work of Rzepecki *et al*. (1986), in which repeat distances were dramatically increased by the protein, the b_5:phospholipid mass ratio was 1, which is similar to the mass ratio of 0.9 for our P450 proteoliposomes. Therefore, we clearly have enough protein present to detect any protein-induced perturbation of membrane structure. Second, one can calculate the expected surface coverage by P450 molecules according to the single membrane-spanning helix model. An ensemble of 1 membrane-bound helix and 90 phospholipid molecules would have a total surface area of *ca*. 6400 Å^2, since the surface area contributed by a single phospholipid molecule is about 70 Å^2 (Lewis & Engelman, 1983), while the cross-sectional area of an α-helix (diameter *ca*. 10 Å) is about 80 Å^2. The surface area of the P450 triangle hypothetically sitting atop the membrane ensemble would be *ca*. 3600 Å^2. Therefore, if the single transmembrane helix model were correct, the P450 heme domain would have covered more than half the surface of our proteoliposomes, and artificially low estimates of *d* due to extensive sagging of the membrane would not be possible.

Finally, we can address the question of which membrane mass distributions can account for the observed small increase in *d*-space compared to the lipid bilayer alone. In Figure 10, three variations of a deeply immersed P450 in the membrane of the stacked multilayers are presented. If the P450 molecules had been incorporated vectorially into the original liposomes so that the protein resided asymmetrically in the bilayer, then the stacked multilayers should give a pattern of alternating projection of the protein up and down in successive bilayers (Figure 10A). As with the multilayers from b_5, the one-dimensional unit cell would consist of two centrosymmetric bilayers, and *d* could not be less than 120 Å. Thus, asymmetric incorporation as in Figure 10A cannot be correct. A variant of asymmetric incorporation is shown in Figure 10B. In this case, while the P450 molecules are incorporated vectorially, the difference from true symmetry is small, so that at the level of resolution provided by our data the incorporation is "pseudosymmetric". Figure 10B shows two electron-dense structural features to account for the maxima at ±8 Å from the center of the bilayer, which may be due to a strong X-ray scatterer associated with the protein. However, it is unlikely that a single P450 molecule would have two well-defined electron-dense regions symmetrically disposed about the center of the bilayer.

If the P450 molecules had been incorporated symmetrically into the original liposomes so that the protein was equally likely to enter the membrane from either side, then the stacked multilayers should give the pattern shown in Figure 10C. While both Figure 10B and Figure 10C predict a *d* similar to a single-bilayer thickness, the symmetric incorporation model in Figure 10C is most in accord with the observed electron density profile. The symmetry of the electron density maxima around the bilayer center is a natural consequence of the P450 being incorporated into the membrane with equal frequency from both directions.

In summary, the observed small increase in *d* of P450-loaded stacked multilayers compared to lipid-only multilayers requires that the protein molecules be deeply immersed. This conclusion was confirmed by the mass distribution profile, which showed that the extra mass due to protein was located only within the bilayer, not substantially outside the bilayer. It should be noted that these conclusions presently apply only to P450 2B4; other microsomal P450 enzymes may have different modes of association with the membrane.

ACKNOWLEDGMENT

We are grateful to Ms. Connie Christian and Dr. Leslie Cutler of the University of Connecticut Health Center for assistance in obtaining the electron micrographs, to Dr. David Chester of the Biomolecular Structure Analysis Center for advice on obtaining and analyzing X-ray diffraction patterns, to Dr. Klaus Gawrisch of the Laboratory for Membrane Biochemistry and Biophysics of the National Institutes of Health for scientific discussion of our results, and to Dr. Terry Stouch of the Bristol-Myers Squibb Pharmaceutical Research Institute for helpful discussions about membrane structure.

REFERENCES

Arinç, E., Rzepecki, L. M., & Strittmatter, P. (1987) *J. Biol. Chem. 262*, 15563−15567.

Barenholtz, Y., Gibbes, D., Litman, B. J., Goll, J., Thompson, T. E., & Carlson, F. D. (1977) *Biochemistry 16*, 2806−2810.

Black, S. D., Martin, S. T., & Smith, C. A. (1994) *Biochemistry 33*, 6945−6951.

Bosterling, B., Stier, A., Hildebrandt, A. G., Dawson, J. H., & Trudell, J. R. (1979) *Mol. Pharmacol. 16*, 332−342.

Brown, C. A., & Black, S. D. (1989) *J. Biol. Chem. 264*, 4442−4449.
Chen, P. S., Jr., Toribara, T. Y., & Warner, H. (1956) *Anal. Chem. 28*, 1756−1758.
Coon, M. J., van der Hoeven, T. A., Dahl, S. A., & Haugen, D. A. (1978) *Methods Enzymol. 52*, 109−117.
DePierre, J. W., & Dallner, G. (1975) *Biochim. Biophys. Acta 415*, 411−472.
Edwards, R. J., Murray, B. P., Singleton, A. M., & Boobis, A. R. (1991) *Biochemistry 30*, 71−76.
Enoch, H. G., & Strittmatter, P. (1978) *Proc. Natl. Acad. Sci. U.S.A 76*, 145−149.
Franks, N. P., & Lieb, W. R. (1981) in *Liposomes: From Physical Structure to Therapeutic Applications* (Knight, C. G., Ed.) pp 243−272, Elsevier/North-Holland Biomedical Press, Amsterdam.
Geurts van Kessel, W. S. M., Hax, W. M. A., Demel, R. A., & De Gier, J. (1977) *Biochem. Biophys. Acta 486*, 524−530.
Gut, J., Richter, C., Cherry, R. J., Winterhalter, K. H., & Kawato, S. (1982) *J. Biol. Chem. 257*, 7030−7036.
Hasemann, C. A., Kurumbail, R. G., Boddupali, S. S., Peterson, J. A., & Deisenhofer, J. (1995) *Structure 2*, 41−62.
Heineman, F. S., & Ozols, J. (1982) *J. Biol. Chem. 257*, 14988−14999.
Herbette, L., Marqaurdt, J., Scarpa, A., & Blasie, J. K. (1977) *Biophys. J. 20*, 245−272.
Herbette, L., Scarpa, A., Blasie, J. K., Wang, C. T., Hymel, L., Seelig, J., & Fleischer, S. (1983) *Biochim. Biophys. Acta 730*, 369−378.
Herbette, L. G., MacAlister, T., Ashavaid, T. F., & Colvin, R. A. (1985) *Biochim. Biophys. Acta 812*, 609−623.
Ingelman-Sundberg, M. (1986) in *Cytochrome P-450. Structure, Mechanism, & Biochemistry* (Oritz de Montellano, P. R., Ed.) pp 119−160, Plenum Press, New York.
Kominami, S., Tagashira, H., Ohta, Y., Yamada, M., Kawato, S., & Takemori, S. (1993) *Biochemistry 32*, 12935−12940.
Kunz, B. C., Vergères, G., Winterhalter, & Richter, C. (1991) *Biochim. Biophys. Acta 1063*, 226−234.
Lewis, B. A., & Engelman, D. M. (1983) *J. Mol. Biol. 166*, 211−217.
McCarthy, M.-B., & White, R. E. (1983) *J. Biol. Chem. 258*, 9153−9158.
Nelson, D. R., & Strobel, H. W. (1988) *J. Biol. Chem. 263*, 6038−6050.
Nelson, D. R., Kamataki, T., Waxman, D. J., Guengerich, F. P., Estabrook, R. W., Feyereisen, R., Gonzalez, F. J., Coon, M. J., Gunsalus, I. C., Gotoh, O., Okuda, K., & Nebert, D. W. (1993) *DNA Cell. Biol. 12*, 1−51.
Ohta, Y., Kawato, S., Tagashira, H., Takemori, S., & Kominami, S. (1992) *Biochemistry 31*, 12680−12687.
Ohta, Y., Sakaki, T., Yabusaki, Y., Ohkawa, H., & Kawato, S. (1994) *J. Biol. Chem. 269*, 15597−15600.
Pachence, J. M., Dutton, P. L., & Blasie, J. K. (1979) *Biochim. Biophys. Acta 548*, 348−373.
Pernecky, S. J., Olken, N. M., Bestervelt, L. L., & Coon, M. J. (1995) *Arch. Biochem. Biophys. 318*, 446−456.
Rzepecki, L. M., Strittmatter, P., & Herbette, L. G. (1986) *Biophys. J. 49*, 829−838.
Schwarz, D., Pirrwitz, J., Meyer, H. W., Coon, M. J., & Ruckpaul, K. (1990) *Biochem. Biophys. Res. Commun. 171*, 175−181.
Seybert, D. W., Lancaster, J. R., Jr., Lambeth, J. D., & Kamin, H. (1979) *J. Biol. Chem. 254*, 12088−12098.
Skidmore, W. D., & Entenman, C. (1962) *J. Lipid Res. 3*, 471−475.
Szoka, F., Olson, F., Heath, T., Vail, W., Mayhew, E., & Papahadjopoulos, D. (1980) *Biochim. Biophys. Acta 601*, 559−571.
Takemori, S., & Kominami, S. (1984) *Trends Biochem. Sci. 9*, 393−396.
Tarr, G. E., Black, S. D., Fujita, V. S., & Coon, M. J. (1983) *Proc. Natl. Acad. Sci. U.S.A. 80*, 6552−6556.
Uvarov, V. Y., Sotnichenko, A. I., Vodovozova, E. L., Molotkovsky, J. G., Kolesanova, E. F., Lyulkin, Y. A., Stier, A., Krueger, V., & Archakov, A. I. (1994) *Eur. J. Biochem. 222*, 484−489.
Vergères, G., Winterhalter, K. H., & Richter, C. (1991) *Biochim. Biophys. Acta 1063*, 235−241.
White, R. E., & Coon, M. J. (1982) *J. Biol. Chem. 257*, 3073−3083.

BI9514572